PHYSICAL REVIEW B VOLUME 18, NUMBER 5 1 SEPTEMBER 1978

Calculated cross sections for elastic scattering of neutrons from vortex rings in liquid ^{4}He

Charles J. Morgan* and H. W. Jackson†
Department of Physics, Washington University, St. Louis, Missouri 63130

S. A. Werner
Department of Physics, University of Missouri, Columbia, Missouri 65201
(Received 16 August 1976; revised manuscript received 18 July 1977)

A theory of elastic scattering of neutrons from vortex rings in liquid ^{4}He is presented, and a study is made of the dependence of the differential cross section on the parameters that characterize the vortices. The sensitivity of the cross section to the details of the density profile in and near the vortex core is examined with the aid of numerical calculations based on simple models. The usefulness and significance of these calculations with regard to recent theoretical work on liquid ^{4}He near the λ point and also with regard to liquid ^{4}He turbulence produced by intense heat fluxes or ion beams is discussed.

I. INTRODUCTION

Recent work on the theory of liquid ^{4}He suggests that quantized vortex rings may start to condense spontaneously at temperatures somewhat below T_λ and that their number density may be large at elevated temperatures.[1] The significance of such a phenomenon, if it actually exists, is that it would provide a mechanism that might be responsible for the specific-heat anomaly at T_λ. Since the basic theory of the vortex condensation involves an element of speculation at the present time, and it seems unlikely that the remaining problems will be settled decisively by theory alone in the very near future, it appears that an experimental study of the situation would serve a highly useful purpose. These considerations provide the principal motivation for carrying out the calculations reported here. However, the computed results would also be applicable to experiments designed to study the possibility that vortex rings are present in liquid-helium turbulence that has been produced by high-intensity heat fluxes or ion beams. Part of the theory developed here could also serve as the starting point for calculations dealing with other assumed vortex configurations, e.g., a tangle of vortex lines. Both Onsager[2] and Feynman[3] have speculated that such a phenomenon might exist in He I.

In the theory developed here, the mechanism responsible for the scattering is the coupling of the incident neutrons to density variations in the vicinity of the vortex cores. Cross sections for elastic scattering of thermal neutrons from vortex rings in liquid ^{4}He are calculated, and features of the cross sections that are characteristic of rings of a given size and core radius are discussed. Three simple models for the density profiles in and near the vortex cores are studied. The main conclusions drawn here are of a qualitative nature and are contained in the statements that measurable elastic cross sections may be associated with vortex structures and that neutron scattering is a promising method for producing direct evidence of these structures.

II. DERIVATION OF FORMULAS FOR ELASTIC CROSS SECTIONS

According to the theory of Van Hove,[4] the differential scattering cross section can be written

$$\frac{d^2\sigma}{d\Omega\, dE_f} = \frac{\sigma_b}{4\pi\hbar}\frac{k_f}{k_i} S(\vec{Q},\omega) \quad , \tag{1}$$

where σ_b is the bound-atom cross section, and k_i and k_f are wave vectors of particles in the incident and scattered beams, respectively. The dynamic structure function $S(\vec{Q},\omega)$ is given by

$$S(\vec{Q},\omega) = \sum_{l,m} p_l \left|\langle m | \sum_{1\le j\le N} e^{i\vec{Q}\cdot\vec{x}_j} | l\rangle\right|^2 \delta(\omega-\omega_{ml}) \quad , \tag{2}$$

where p_l is the probability for the lth state. Since we are concerned with elastic scattering, our attention will be focused just on the diagonal matrix elements $(l=m)$ in Eq. (2). Denoting the elastic part of the structure function by $S_0(\vec{Q},\omega)$, and introducing the one-particle distribution function

$$n_l(\vec{x}_1) = N\int d^3x_2 \cdots d^3x_N\, |\psi_l(\vec{x}_1,\ldots,\vec{x}_n)|^2 \quad , \tag{3}$$

one can write

$$S_0(\vec{Q},\omega) = \delta(\omega)\sum_l p_l \left|\int d^3x\, e^{i\vec{Q}\cdot\vec{x}} n_l(\vec{x})\right|^2 \quad . \tag{4}$$

For the liquid at 0 °K, the wave function that corresponds to a single rectilinear vortex bearing one quantum unit of circulation can be written approximately in the form[1,5]

$$\psi(\vec{x}_1, \ldots, \vec{x}_N) = \psi_0(\vec{x}_1, \ldots, \vec{x}_N) \times \prod_{1\le j\le N} P(\rho_j) e^{i\theta_j} , \quad (5)$$

where ρ_j and θ_j are polar coordinates measured with respect to the vortex center. In Eq. (5), ψ_0 is the wave function for the liquid in its ground state, without a vortex, and it is an eigenfunction of the z component of angular momentum with eigenvalue zero. The factors $e^{i\theta_j}$ account for the characteristic velocity field of a quantized vortex, and the factors of $P(\rho_j)$ account for the variations in the density near the center of the vortex. Excited-state wave functions ψ', involving phonons and rotons, include the function ψ of Eq. (5) as a factor when a single vortex is present. The variation in the density is still determined mainly by the function ψ, and so we shall deal only with that function in our calculations. This procedure can be justified formally by simply interpreting the quantity p_l in Eq. (4) as the probability for all states having the same vortex structure, but having different numbers of phonons and rotons. The wave function for a collection of vortex lines can be built up from the simple one in Eq. (5) by including additional factors of $P(\rho)$ and $e^{i\theta}$ with ρ and θ measured with respect to appropriate origins. Simple modifications of these formulas can be made in order to adapt them to vortex rings. For a single vortex whose center is at the origin of the coordinate system, the wave function is

$$\psi(\vec{x}_1, \ldots, \vec{x}_N) = \psi_0(\vec{x}_1, \ldots, \vec{x}_N) \times \prod_{1\le j\le N} R(\vec{x}_j) e^{iT(\vec{x}_j)} , \quad (6)$$

where $R(\vec{x})$ and $T(\vec{x})$ are certain real valued functions of $\vec{x}$. For N' similar vortex rings whose cores do not overlap, the wave function is

$$\psi_l(\vec{x}_1, \ldots, \vec{x}_N) = \psi_0(\vec{x}_1, \ldots, \vec{x}_N) \times \prod_{1\le j\le N} \prod_{1\le\alpha\le N'} R_l(\vec{r}_{j\alpha}) e^{iT_l(\vec{r}_{j\alpha})} . \quad (7)$$

where l is a label associated with a particular configuration of the vortices. Notice that the sum in Eq. (4) may be limited to those states for which $p_l \neq 0$, viz., the vortex ring states, in the situations that we are considering. In Eq. (7), we have used the notation

$$\vec{r}_{j\alpha} = \vec{x}_j - \vec{y}_\alpha , \quad (8)$$

where $\vec{y}_\alpha$ locates the center of the vortex ring labeled by α. As a practical matter, we are supposing that all of the rings are the same size. This should lead to useful results provided that the actual distribution of sizes about the average is fairly sharply peaked. Taking the square modulus of ψ_l in Eq. (7) and inserting the result into Eq. (3), we find the following formula for n_l:

$$n_l(\vec{x}_1) = N \int d^3x_2 \cdots d^3x_N \, |\psi_0(\vec{x}_1, \ldots, \vec{x}_N)|^2 \times \prod_{1\le j\le N} \prod_{1\le\alpha\le N'} R_l^2(\vec{x}_j - \vec{y}_\alpha) . \quad (9)$$

To proceed further, we must approximate the right-hand side of Eq. (9). To justify the method that we shall use here, let us first consider a simple situation in which a single rectilinear vortex is located on the z axis. Then one can express $n_l(\vec{x}_1)$ in a form analogous to Eq. (9) by using Eqs. (3) and (5). Taking the gradient with respect to the coordinates of particle 1 of the ensuing equation, one obtains a differential equation for $\nabla_1 n_l(\vec{x}_1)$. That equation has been solved approximately in Ref. 1, and there it was found that a zeroth order solution is

$$n_l(\vec{x}_1) = nP_l^2(\rho_1) , \quad (10)$$

where ρ_1 is a cylindrical radial coordinate, and n is the average number density of particles. That is, the factor P in the wave function is simply proportional to the square root of the number density in this approximation. In the reference cited, it was found that corrections to this result are small, and so for our purposes here it should be sufficiently accurate. A straightforward extension of that method to a collection of N' rectilinear vortices gives

$$n_l(\vec{x}_1) = n \prod_{1\le\alpha\le N'} P_l^2(\rho_{1\alpha}) . \quad (11)$$

Adapting this result to a collection of vortex rings, we have

$$n_l(\vec{x}_1) = n \prod_{1\le\alpha\le N'} R_l^2(\vec{x}_1 - \vec{y}_\alpha) . \quad (12)$$

The Fourier transform of $n_l(\vec{x})$ can be calculated most easily by first introducing hole functions $h_l(\vec{r}_{1\alpha})$ through the relation

$$h_l(\vec{r}_{1\alpha}) = R_l^2(\vec{r}_{1\alpha}) - 1 , \quad (13)$$

where we have assumed that $R_l(\vec{r}_{1\alpha})$ has the value unity except in and near the vortex core. For configurations in which the hole functions of different vortex rings do not overlap, the product in Eq.(12) can be converted to the sum

$$n_l(\vec{x}_1) = n\left[1 + \sum_{1\le\alpha\le N'} h_l(\vec{r}_{1\alpha})\right] . \quad (14)$$

For $\vec{Q} \neq 0$, Eq. (14) enables us to rewrite Eq. (4) as

$$S_0(\vec{Q},\omega)=\delta(\omega)\sum_l p_l\left|\sum_{1\le\alpha\le N'} e^{i\vec{Q}\cdot\vec{y}_\alpha}\times\int d^3r_{1\alpha}e^{i\vec{Q}\cdot\vec{r}_{1\alpha}}nh_l(\vec{r}_{1\alpha})\right|^2 . \tag{15}$$

In Eq. (15), p_l assigns a statistical weight to each configuration characterized by the spatial location and angular orientation of each vortex in the liquid. In this paper, we shall assume that p_l can be written as the product of two independent weights, p_R and p_S :

$$p_l=p_Rp_S . \tag{16}$$

The subscript R refers to rotational degrees of freedom, whereas the subscript S refers to the spatial arrangements of the centers of the rings.

Now we want to calculate the angular dependence of $S_0(\vec{Q},\omega)$ in Eq. (15). Let $F_l(\vec{Q})$ denote the Fourier transform of the hole function for a given density profile; then

$$F_l(\vec{Q})=n\int d^3r\, e^{i\vec{Q}\cdot\vec{r}}h_l(\vec{r}) . \tag{17}$$

The orientation of this profile can be related to that of a reference profile h_0 by specifying two Euler angles, ϕ and θ. Then introducing the rotation operator

$$R=R(\phi,\theta) , \tag{18}$$

the correspondence between h_l and h_0 can be expressed as

$$h_l(\vec{r})=h_0(R\vec{r}) . \tag{19}$$

Next, the invariance of the scalar product under rotations gives

$$\vec{Q}\cdot\vec{r}=(R\vec{Q})\cdot(R\vec{r}) . \tag{20}$$

From Eqs. (17)–(20) it follows that

$$F_l(\vec{Q})=F_0(R\vec{Q}) . \tag{21}$$

This procedure can be generalized to deal with Eq. (15) by introducing a set of N' rotation operators

$$R_\alpha=R(\phi_\alpha,\theta_\alpha),\quad \alpha=1,\ldots,N' , \tag{22}$$

which specify the relative orientation of each ring in the fluid for the configuration labeled l. Then Eq. (15) becomes

$$S_0(\vec{Q},\omega)=\delta(\omega)\sum_S p_S\sum_R p_R\left|\sum_{1\le\alpha\le N'} e^{i\vec{Q}\cdot\vec{y}_\alpha}F_0(R_\alpha\vec{Q})\right|^2 . \tag{23}$$

Let us use angular brackets to denote the average for a single ring over its available orientations, and introduce the N'-point distribution function $p_S(\vec{y}_1,\vec{y}_2,\ldots,\vec{y}_{N'})$ to describe the distribution of ring centers in the liquid. Then Eq. (23) can be rewritten

$$S_0(\vec{Q},\omega)=\delta(\omega)\int d^3y_1\cdots d^3y_{N'}\,p_S(\vec{y}_1,\ldots,\vec{y}_{N'})\left[N'\langle|F_0(\vec{Q})|^2\rangle+|\langle F_0(\vec{Q})\rangle|^2\sum_{\substack{\alpha,\beta\\(\alpha\neq\beta)}}e^{i\vec{Q}\cdot(\vec{y}_\alpha-\vec{y}_\beta)}\right] . \tag{24}$$

Paralleling procedures used in the theory of ordinary liquids, we shall define a "vortex structure factor," analogous to a static liquid structure factor. In order to do that, we let $D=N'/V$ be the number density for vortex rings, and define a vortex pair correlation function as

$$G(\vec{y}_1-\vec{y}_2)=\frac{N'(N'-1)}{D^2}\int d^3y_3\,d^3y_4\cdots d^3y_{N'}\,p_S(\vec{y}_1,\vec{y}_2,\ldots,\vec{y}_{N'}) . \tag{25}$$

Finally, the vortex structure factor is given by

$$S_v(\vec{Q})=1+D\int d^3y\,[G(\vec{y})-1]e^{i\vec{Q}\cdot\vec{y}} . \tag{26}$$

With the aid of $S_v(\vec{Q})$, we can now rewrite Eq. (24) as

$$S_0(\vec{Q},\omega)=\delta(\omega)N'\{[\langle|F_0(\vec{Q})|^2\rangle-|\langle F_0(\vec{Q})\rangle|^2]+|\langle F_0(\vec{Q})\rangle|^2S_v(\vec{Q})\} . \tag{27}$$

Equation (27) contains the main result of this section. In essence, it gives the cross section for elastic scattering of neutrons directly in terms of the diffraction properties of the vortex core density profile. The form of $S_v(\vec{Q})$ to be used in Eq. (27) will depend, in general, on the vortex distribution being considered.

We will apply Eq. (27) to two specific models involving qualitatively different spatial distributions. One is a "vortex gas" in which the rings are in spatial configurations describable by a smeared out pair distribution function. The other is a "vortex solid" in which the ring centers lie on a simple lattice.

For the gas model we will use a phenomenological pair distribution function, involving a single Gaussian; then provided that the spatial arrangement of widely separated vortex pairs are uncorrelated we have

$$G(r)=1-e^{-\alpha r^2} . \tag{28}$$

The corresponding vortex structure factor can be evaluated analytically, and is given by the formula

$$S_v(\vec{Q}) = 1 - (\pi/\alpha)^{3/2} D\, e^{-Q^2/4\alpha} \ . \tag{29}$$

This should provide a reasonable model for the vortex distribution in Jackson's theory, as well as in turbulent ^{4}He. For the gas model, the cross section for elastic scattering of neutrons per helium atom in the target is

$$\left(\frac{d^2\sigma}{d\Omega\, dE_f}\right)_0 = \delta(\omega)\frac{\sigma_b}{4\pi\hbar}\left(\frac{N'}{N}\right)\left[\langle|F_0(\vec{Q})|^2\rangle - \left(\frac{\pi}{\alpha}\right)^{3/2} D\,|\langle F_0(Q)\rangle|^2 e^{-Q^2/4\alpha}\right] \ . \tag{30}$$

The lattice model is discussed here because it is tractable mathematically and represents a definite possibility which may be realized when the vortex number density becomes sufficiently great. For a simple cubic lattice containing N' vortex sites and characterized by reciprocal lattice vectors $\vec{G}$, the vortex structure factor is

$$S_v(\vec{Q}) = N'\delta_{\vec{Q},\vec{G}} \ . \tag{31a}$$

Therefore, the elastic cross section per helium atom for this case is

$$\left(\frac{d^2\sigma}{d\Omega\, dE_f}\right)_0 = \delta(\omega)\frac{\sigma_b}{4\pi\hbar}\left(\frac{N'}{N}\right)[\langle|F_0(\vec{Q})|^2\rangle + (N'\delta_{\vec{Q},\vec{G}} - 1)|\langle F_0(\vec{Q})\rangle|^2] \ . \tag{31b}$$

As a practical matter, in representing numerical results of calculation, the factor of $\delta(\omega)$ in Eqs. (30) and (31b) must be omitted. This can be treated formally by introducing a quantity $(d\sigma/d\Omega)_0$, the angular distribution for elastic scattering, which is defined in the following way:

$$\left(\frac{d\sigma}{d\Omega}\right)_0 = \int_{-\epsilon}^{\epsilon} \hbar\, d\omega \left(\frac{d^2\sigma}{d\Omega\, dE_f}\right)_0 \tag{32}$$

for $\epsilon > 0$.

The quantitative implications of Eqs. (27) and (31b) can be understood more fully if one analyzes the properties of the vortex form factor $F_0(Q)$. That analysis has been carried out, in part by numerical methods, for a range of ring and core radii and for three different models of the core structure. The three models that have been considered are: (i) a hollow core embedded in a uniform background; (ii) a smoothly varying density profile that is zero only at the center of the core; and (iii) a hollow core surrounded by a mantle of constant, high density, embedded in a uniform background. The deficiency of atoms in the core is exactly compensated by the excess of atoms in the mantle. Results for these models are discussed in Sec. III.

III. EVALUATION OF THE VORTEX FORM FACTOR $F_0(\vec{Q})$ AND DISCUSSION OF RESULTS

First we will consider the case of a hollow toroidal core embedded in a uniform background of particle density n. A cross sectional view of the torus in a plane containing the symmetry axis is shown in Fig. 1. In cylindrical coordinates, the equation for the surface of a torus having core radius A and ring radius B is given by

$$(\rho - B)^2 + z^2 = A^2, \quad |\rho - B| \le A \ . \tag{33}$$

Referring to Eq. (17) and taking l to refer to the standard orientation 0 for the present, we can write

$$F_0(\vec{Q}) = -n \int\int_{|\rho - B| \le A} dx\, dy\, e^{i(Q_1 x + Q_2 y)} \times \int_{-z_0}^{z_0} dz\, e^{iQ_3 z} \ , \tag{34}$$

where

$$z_0 = [A^2 - (\rho - B)^2]^{1/2} \ . \tag{35}$$

Because of the axial symmetry of the torus, it is helpful to express the x and y components of vectors in polar form using complex variable notation. Then

$$x + iy = \rho e^{i\phi}, \quad Q_1 + iQ_2 = Ke^{i\psi} \ . \tag{36}$$

The first exponential in Eq. (34) can be expanded in the following orthogonal series (Jacobi-Anger formula):

$$e^{i(Q_1 x + Q_2 y)} = \sum_{-\infty \le n \le \infty} (ie^{i\psi})^n J_n(k\rho) e^{im\phi} \ , \tag{37}$$

where J_n is the Bessel function of order n. Substituting this into Eq. (34) and performing the integrations over the angle ϕ and coordinate z gives

$$F_0(\vec{Q}) = -\frac{4\pi n}{Q_3}\int_{B-A}^{B+A} d\rho\, \rho J_0(k\rho) \times \sin\{Q_3[A^2 - (\rho - B)^2]^{1/2}\} \ . \tag{38}$$

In the cross-section formula derived earlier, this function occurs in a statistical average. If the weights p_R are such that the rings all have a single orientation,

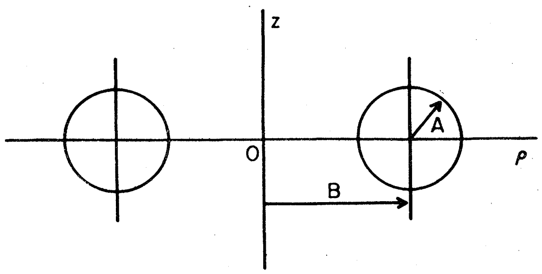

FIG. 1. Coordinate system for a vortex ring, where $\rho=(x^2+y^2)^{1/2}$.

then Eq. (38) can be applied directly. However, when the vortices form spontaneously near the λ point or when they are generated in turbulent helium, it is probably more realistic to suppose that all orientations are equally likely. In this case, $F_0(\vec{Q})$ and $|F_0(\vec{Q})|^2$ must be averaged over the angles θ and ϕ shown in Fig. 2. In general, those average values cannot be expressed in a simple analytic form but must be evaluated numerically. However, it is possible to obtain an analytic expression for $\langle F_0(\vec{Q})\rangle$ whenever B is much larger than A, and this gives some insight into the structure of the scattering cross section.

To average $F_0(\vec{Q})$ over a sphere, first make the transformation

$$Q_3^{-1}\sin\{Q_3[A^2-(\rho-B)^2]^{1/2}\}=\int_0^{[A^2-(\rho-B)^2]^{1/2}} dt\cos(Q_3t) \quad . \tag{39}$$

Once again we introduce polar coordinates in complex variable notation, and write

$$Q_3+iK=Qe^{i\theta} \quad . \tag{40}$$

When Eqs. (39) and (40) are combined with (38) and the average over all solid angles is taken, one gets

$$\langle F_0(\vec{Q})\rangle=-2\pi n\int_{B-A}^{B+A} d\rho\,\rho\int_0^{[A^2-(\rho-B)^2]^{1/2}} dt\int_0^{\pi} d\theta\sin\theta\, J_0(Q\rho\sin\theta)\cos(Qt\cos\theta) \tag{41a}$$

$$=-\frac{4\pi n}{Q}\int_{B-A}^{B+A} d\rho\,\rho\int_0^{[A^2-(\rho-B)^2]^{1/2}} dt\,\frac{\sin[Q(\rho^2+t^2)^{1/2}]}{(\rho^2+t^2)^{1/2}} \quad . \tag{41b}$$

An evaluation of the integral over the angle θ is given in the Appendix. Equation (41b) can be further simplified by interchanging the order of integration. The new limits can be deduced easily with the aid of Fig. 3, where the shaded region that constitutes the interior of a semicircle defines the domain of integration. This procedure gives

$$\langle F_0(\vec{Q})\rangle=-\frac{4\pi n}{Q}\int_0^{A} dt\int_{B-(A^2-t^2)^{1/2}}^{B+(A^2-t^2)^{1/2}} d\rho\times\rho\frac{\sin[Q(\rho^2+t^2)^{1/2}]}{(\rho^2+t^2)^{1/2}} \quad . \tag{42}$$

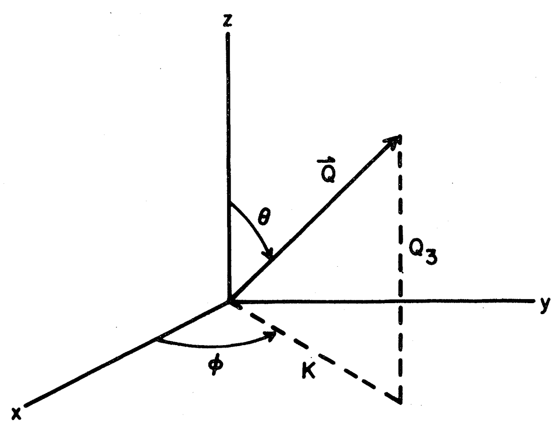

FIG. 2. Defining representation of the Euler angles θ and ϕ and the components K and Q_3 of the momentum transfer $\vec{Q}$. The z axis coincides with that in Fig. 1.

Finally, introducing new variables of integration u and w, through the relations

$$u=(\rho^2+t^2)^{1/2},\quad t=A\sin w \quad , \tag{43}$$

one can reduce Eq. (42) to

$$\langle F_0(\vec{Q})\rangle=-(4\pi^2A/Q^2)n\sin(QB)J_1(QA)\quad \text{for} A/B \ll 1 \quad . \tag{44}$$

Comparing this with results obtained by numerical integration methods, one finds that the formula in Eq. (44) holds quite well for A/B as large as 0.3. The right-hand side of Eq. (44) divided by n tends to the volume of a torus as $Q\rightarrow 0$; this provides a useful check on the formula in Eq. (44). Thus,

$$\lim_{Q\rightarrow 0}\frac{1}{n}|\langle F_0(\vec{Q})\rangle|=2\pi^2A^2B \quad . \tag{45}$$

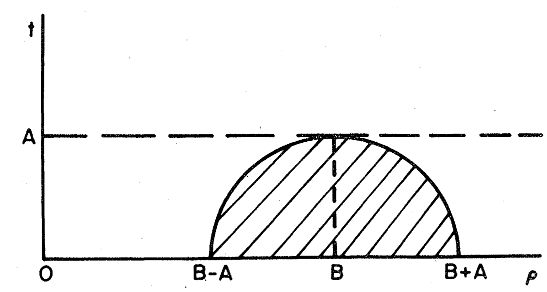

FIG. 3. Representation of the domain of integration, viz. the shaded region, for Eqs. (41b) and (42).

The usefulness of these formulas will become clear shortly.

Consider Fig. 4, which shows the calculated cross section for neutrons elastically scattered from a gas of vortices characterized by a hollow core with radius $A = 3.0$ Å, a ring radius of $B = 10.0$ Å, a mean density of $D = (40.0\text{Å})^{-3}$, and a correlation length of $\alpha^{-1/2} = 20.0$ Å. In all calculations reported here, we have assumed $\sigma_b = 1.13$ b. The maximum value of the cross section occurs near $Q = 0.1$ Å^{-1} and the peak value is about 100 b/sr per helium atom. From Eq. (31b) and Fig. 5 one can infer that changes in $\langle |F_0(\vec{Q})|^2 \rangle$ as a function of Q follow closely the changes in the envelope of $|\langle F_0(\vec{Q})\rangle|^2$. From this observation and Eq. (44), one can deduce that the core radius A largely governs the range of Q for which elastic scattering is appreciable; whereas the ring radius B largely controls the fine structure in the elastic scattering cross section. Even when the vortices are modeled more realistically, these observations still seem to be valid. Therefore they should be useful in analyzing experimental data if elastic scattering from liquid ^{4}He is observed.

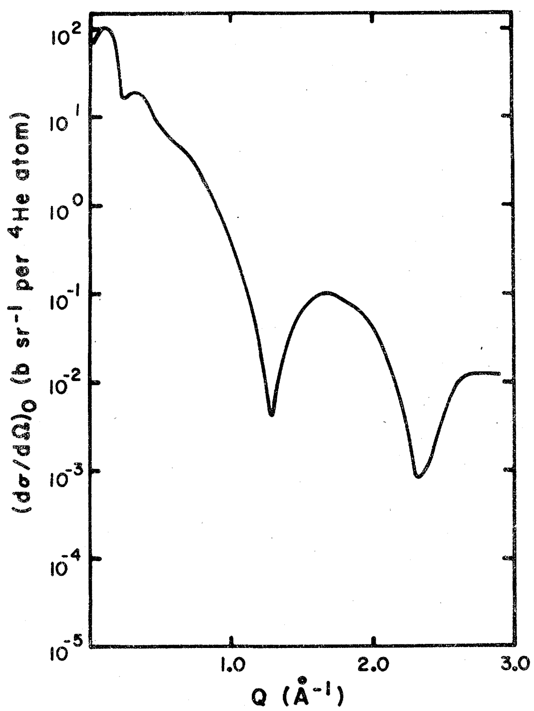

FIG. 4. Plot of the cross section $(d\sigma/d\Omega)_0$, for elastic scattering of neutrons from a gas of hollow vortex rings vs momentum transfer Q based on Eqs. (30) and (32). All orientations of the rings are taken to be equally likely. The ring radius of the vortices is 10.0 Å, the core radius is 3.0 Å, the mean density of vortices is (40.0 Å)$^{-3}$, and the correlation length $\alpha^{-1/2}$ is 20.0 Å.

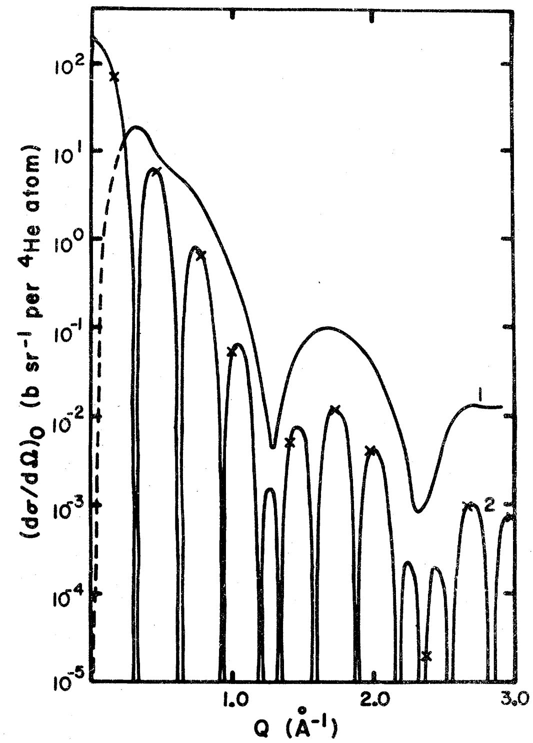

FIG. 5. Plot of the cross section $(d\sigma/d\Omega)_0$ for elastic scattering of neutrons from hollow vortex rings distributed on a cubic lattice, having a primitive translation vector of length 40.0 Å. The curves are based on Eqs. (31b) and (32). The ring and core radii are the same as in Fig. 4. Curve 1 gives the continuous part of the cross section, and curve 2 gives the envelope of the Bragg peaks, except for a factor N', which has been omitted. The Bragg points are denoted by crosses.

Figure 5 shows calculated cross sections for a simple cubic spatial array of vortices with a lattice spacing of 40.0 Å. The vortex parameters A and B are the same as in Fig. 4. Since we have assumed that the number of vortices N' within a macroscopic volume of helium is extremely large, it is not practical to represent the continuous and discrete contributions in Eq. (31b) on the same scale. Therefore, two curves are displayed. Curve 1 gives the continuous part of the cross section, which has a peak value of about 20 b per helium atom. Curve 2 gives, within a factor of N', the envelope of the contribution of the Bragg peaks, the actual Bragg points being denoted by crosses. The structure of curve 2 can be readily understood by referring to Eq. (44).

To study the sensitivity of the computed cross section to the details of the core density profile, we have made further calculations with the more realistic hole function[1]

$$h_0(\rho;z) = \sin^2(\pi R/2A), \quad R \leq A \quad , \tag{46}$$

where ρ and z are defined in Fig. 1, and R measures the radial distance from the core center. The results are shown in Figs. 6 and 7. Although there are discernible changes in features of the cross sections, the gross behavior is the same as in the previous case. The decrease of intensity in the forward peak for the partly filled core is due to the effective reduction of the core volume. Therefore, before directly comparing the scattering intensities associated with the two core models, one should choose a larger radius A in Eq. (46) than for the hollow core.

In the analysis given so far, we have considered only models in which the density of atoms is constant outside of the core regions. Models of this type have been both popular and useful. However, certain calculations indicate that there may be appreciable density variations even outside of the vortex cores. For isothermal conditions, the density would be greater in regions where the superfluid velocity is higher. To investigate the influence of this phenomenon on the elastic scattering cross section, we have made calculations for a model in which a hollow vortex core is surrounded by a mantle of constant high density. The density and radius of the mantle were chosen so that the deficiency of atoms in the core is exactly compensated by the excess of atoms in the mantle. We recognize that this is an extreme assumption, and we do not know of any general principle that requires this

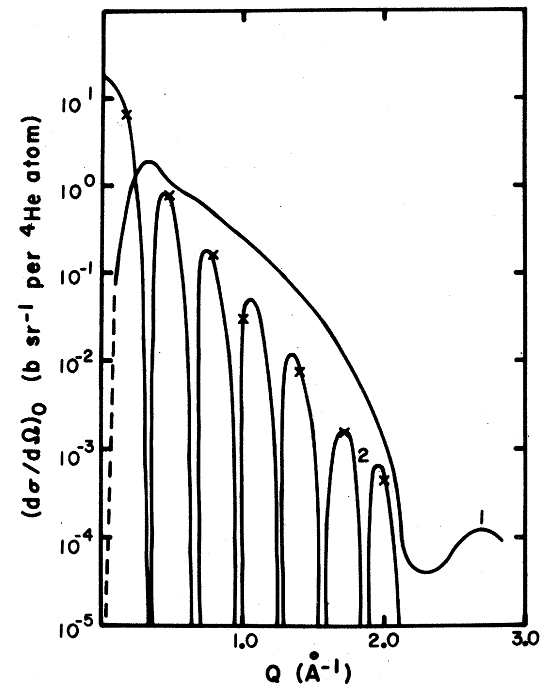

FIG. 7. Plot of elastic cross section $(d\sigma/d\Omega)_0$ vs momentum transfer Q for scattering from vortices characterized by a core profile $h_0(\rho,z)=\sin^2(R\pi/2A)$, $R\leq A$. The other parameters and conditions are the same as for Fig. 5.

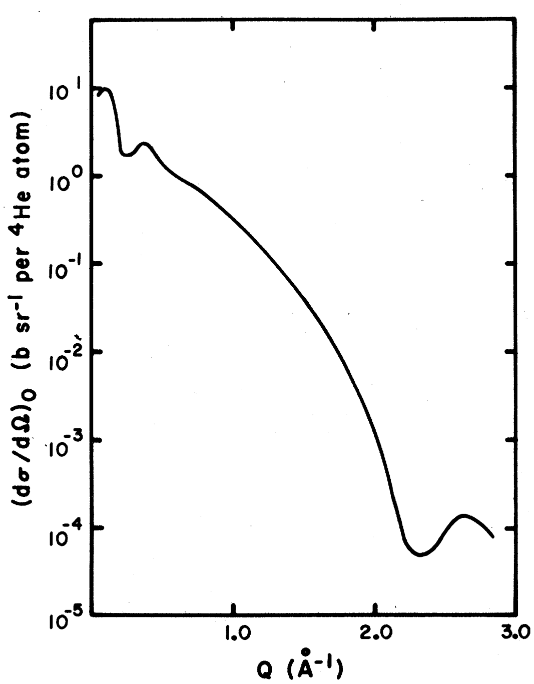

FIG. 6. Plot of elastic scattering cross section $(d\sigma/d\Omega)_0$ vs momentum transfer Q for vortices characterized by a core profile $h_0(\rho,z)=\sin^2(R\pi/2A)$, $R\leq A$. The characteristic parameters are the same as for Fig. 4.

exact compensation. However, the results for this model will enable us to see a trend that is applicable even if the compensation is only partial.

Figure 8 shows the calculated cross section for a gas of vortex rings characterized by the same parameters as in Fig. 4, but with a constant, high-density mantle around the toroidal core. Measured from the center of a core, the region occupied by the mantle is between 3.0 and 5.2 Å. The density there is 0.0327 atoms/Å^3. This density is unrealistically high, being far into the range where the helium would be solid, but we shall use it for illustrative purposes. One feature of the cross section in Fig. 8 that is of central importance now is the steep drop in the cross section as Q tends to zero. From that behavior, one can infer that vortices having the structure assumed here would have little effect in light-scattering experiments, where Q would be of the order of 10^{-3} Å^{-1}. We will comment further on this matter later.

In Fig. 9 are the results for the vortex rings with the same density profile as in Fig. 8, but for a simple cubic spatial array having a lattice spacing of 40.0 Å. Figure 9 should be compared with Figs. 5 and 7. The intensities are still large enough to be easily observable in neutron scattering experiments.

Perhaps we should emphasize that the parameters which characterize the vortex structures in all of our

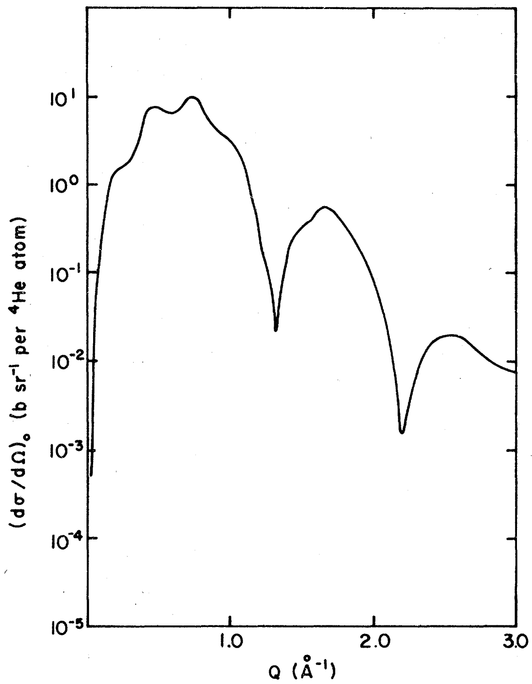

FIG. 8. Plot of elastic scattering cross section $(d\sigma/d\Omega)_0$ vs momentum transfer Q for a gas of vortex rings characterized by a hollow core surrounded by a mantle of constant, high particle density. Measured from the center of a core, the mantle is between 3.0 and 5.2 Å. The particle density there is 0.0327 Å^{-3}. Other characteristic parameters are the same as for Fig. 4.

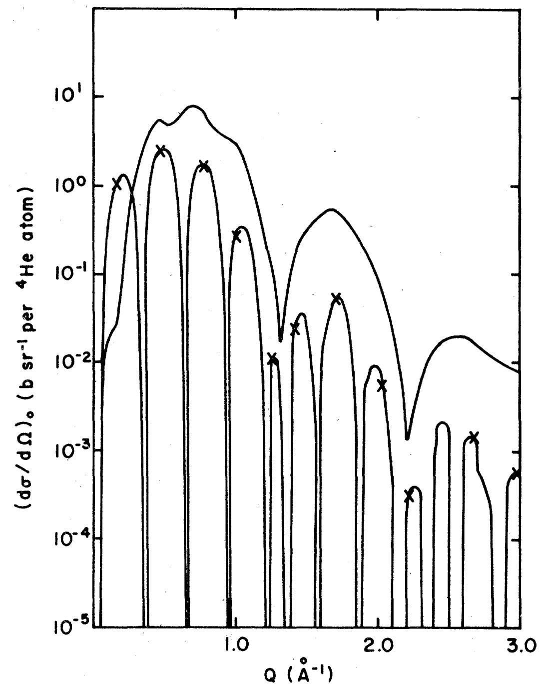

FIG. 9. Plot of elastic cross section $(d\sigma/d\Omega)_0$ vs momentum transfer Q for vortex rings with a constant high-density mantle, distributed on a lattice. The ring characteristics are the same as for Fig. 8; the lattice parameters are the same as for Fig. 5.

calculations were chosen for illustrative purposes. Even though there are some reasons to believe that they may be roughly correct, we should not overlook the possibility that some of those parameters may be wrong even in order of magnitude. Of course, changing the parameters could strongly affect the peak intensities as well as other characteristics of the calculated cross sections. Therefore it is worth noting that even if the peaks in the cross sections are smaller than those in Figs. 8 and 9 by about three orders of magnitude, careful experiments may still be able to detect them. We should also note that the computed cross sections for all models that we have studied are sharply peaked at small values of Q. This indicates that one may have to take special measures to separate scattering events of interest here from those involving the walls of the container and from multiple scattering. For the first two types of the density profile, we have made calculations for several other choices of the vortex parameters, and the results are qualitatively similar to those shown in Figs. 4–7.

A few comments should be made about the feasibility of observing neutrons elastically scattered from externally produced vortex distributions. From observed ion densities in accelerated ion experiments,[6] one can estimate an upper limit on the vortex ring number density to be $D < 10^6$ cm^{-3}. Using the ^{4}He particle density $n = 0.0218$ Å^{-3}, one finds $N'/N < 10^{-16}$. Since this ratio is a multiplicative factor in Eq. (30), it appears unlikely that an elastic cross section will be observable for this case. The small-number density is believed to be due to the fact that the vortices are charged and so their spatial distribution is space-charge limited.

The situation is more favorable for vorticity occurring in helium turbulence. From the data of Phillips and McClintock, Henson[7] has estimated that an upper limit on the length of vortex line per unit volume lies between 5×10^7 and 5×10^{10} mm/mm^3. If this were distributed among vortex rings of mean radius 10.0 Å, then the ratio N'/N would lie between 10^{-7} and 10^{-4}. This term, occurring as a factor in Eq. (30), is large enough for one to consider seriously the possibility of studying the nature of the vorticity in helium turbulence by employing the method of elastic scattering of neutrons. In connection with this last statement, one should note that $N'/N \simeq 10^{-3}$ for the examples treated in detail in this paper.

Now let us return to the subject of vortices spontaneously formed in liquid ^{4}He. In the literature there is a large amount of information on relevant scattering experiments involving light, x rays, and neutrons. Some observations based on a study of those experiments are given below.

Measurements of light scattering from liquid ^{4}He near T_λ, both at saturated vapor pressure and at 25 atm, indicate that there is no appreciable elastic scattering there.[8] This would be consistent with the presence of large numbers of vortices of any size provided that the deficiency of atoms in the cores are compensated by excess atoms within distances that are much smaller than a wavelength of the incident light. Even in the absence of appreciable compensation, it would be consistent with the presence of large numbers of vortices on a lattice provided that the smallest primitive reciprocal lattice vector is much larger than a wave vector for light. This last statement can be understood with the aid of Figs. 5, 7, and 9. The light-scattering experiments show that even near T_λ, it is possible to distinguish clearly between elastic and inelastic scattering for at least some range of small wave vectors. Other experiments[9] indicate that the total intensity of light scattered through an angle of 90° is slightly affected as the temperature of the helium is varied through T_λ.

A large number of experiments involving x-ray scattering from liquid ^{4}He have been reported in the literature.[10–16] Only in the experiments of Tweet[10] have measurements been made for wave vectors below 0.1 Å^{-1}; his data cover the range $0.06 \le Q \le 0.36$ Å^{-1}. Most of his data seem to indicate that there is no anomalously large scattering there as the temperature varies from about 1.5 °K to about 4.16 °K. Tweet mentions that there was a possibility that the liquid was bubbling when the temperature was greater than T_λ. Because of this, one can not reach a firm conclusion regarding evidence for vortices from his measurements there. However, other x-ray studies of liquid ^{4}He above T_λ give no evidence of large cross sections for $0.13 \le Q \le 1.0$ Å^{-1} that might indicate the presence of vortices.[16] A survey of the literature reveals that no x-ray scattering measurements have been reported for temperatures just below T_λ when $0.16 \le Q \le 1.0$ Å^{-1}. These are the conditions which would seem to be most favorable for new experiments designed to search for direct evidence of vortices, as we see from our model calculations and the available experimental data.

In a search of the literature on neutron scattering from liquid ^{4}He, we have found only two measurements of line shapes for temperatures just below T_λ and for $Q \le 1.0$ Å^{-1}. Woods[17] has reported data for $T = 2.05$ °K and $Q = 0.38$ Å^{-1}, and Cowley and Woods[18] have reported data for $T = 2.1$ °K and $Q = 0.72$ Å^{-1}. In neither of those experiments was the elastic scattering from the container subtracted. One can infer from their data that if elastic scattering from the liquid was actually present, then it was not very intense. Furthermore, their data indicate that it would be possible to distinguish between the one-phonon peak and an elastic peak of comparable intensity, at least for the particular conditions of their experiments.

If there were many vortices present in the liquid near T_λ, they would affect the inelastic scattering of neutrons by broadening the line appreciably because of the high, nonuniform superfluid velocities near vortex cores, and because of the high roton densities that would enhance the effects of interactions among excitations there. The frequency of the one-phonon peak could be shifted downward by two effects. First, a high particle density, e.g., in a mantle around the vortex cover, would lower the minimum roton energy; second, a net attractive interaction among rotons would have a similar effect. In fact, estimates indicate that one might explain much of the temperature dependence of inelastic neutron scattering data fairly well if vortices are assumed to be present. However, even in the absence of vortices one might be able to account for the observed scattering lines near T_λ on the basis of certain interactions among elementary excitations alone. Therefore inelastic scattering does not seem to provide a definite, simple test for the existence of vortices, and that is why we have concentrated only on elastic scattering in our study here.

In summary, we conclude from model calculations and from a study of available experimental data that measurement of elastic neutron scattering cross sections is a reasonable method for searching for direct evidence that vortices are present in the liquid at temperatures somewhat below T_λ. The wave-vector range smaller than 1.0 Å^{-1} seems to be the most favorable for this search.

ACKNOWLEDGMENTS

One of the authors (H.W.J.) would like to acknowledge useful discussions with Professor B. L. Henson and Professor F. E. Moss on the subject of turbulence in liquid ^{4}He.

APPENDIX: EVALUATION OF THE ANGULAR INTEGRAL

$$I = \int_0^\pi d\theta \sin\theta\, J_0(Q\rho\sin\theta)\cos(Qt\cos\theta) \quad .$$

From the tables,[19]

$$\int_0^{\pi/2} d\theta \sin\theta\, J_0(z\sin\theta)(\cos\theta)^{2m} = (2/z)^m[\Gamma(m+\tfrac{1}{2})/\sqrt{\pi}]\,j_m(z) \quad , \tag{A1}$$

where $j_m(z)$ is a spherical Bessel function of order m. Therefore, expanding $\cos(Qt\cos\theta)$ in a power series and using Eq. (A1) to integrate term by term, one obtains

$$I=\frac{2}{\sqrt{\pi}}\sum_{m\geqslant 0}\frac{\Gamma(m+\frac{1}{2})}{\Gamma(2m+1)}\left(-\frac{2Qt^2}{\rho}\right)^m j_m(Q\rho) \ . \qquad (A2)$$

Then employing the duplication formula for γ functions

$$\Gamma(m+\tfrac{1}{2})/\Gamma(2m+1)=\sqrt{\pi}4^{-m}/m! \qquad (A3)$$

and the parity property of Bessel functions

$$j_m(ze^{i\pi})=(-1)^m j_m(z) \ , \qquad (A4)$$

we get

$$I=2\sum_{m\geqslant 0}\frac{1}{m!}\left(\frac{Qt^2}{2\rho}\right)^m j_m(Q\rho e^{i\pi}) \ . \qquad (A5)$$

Next, differentiate the generating function[20]

$$\frac{1}{z}\cos[(z^2-2zy)^{1/2}]=\sum_{m\geqslant 0}\frac{y^m}{m!}j_{m-1}(z) \ ,$$

$$|z|>2|y| \ , \qquad (A6)$$

with respect to y. This gives

$$\frac{\sin[(z^2-2zy)^{1/2}]}{(z^2-2zy)^{1/2}}=\sum_{m\geqslant 0}\frac{y^m}{m!}j_m(z) \ . \qquad (A7)$$

Setting $y=Qt^2/2\rho$, $z=-Q\rho$ in Eq. (A7) and comparing the result with Eq. (A5) gives

$$I=(2/Q)\sin[Q(\rho^2+t^2)^{1/2}]/(\rho^2+t^2)^{1/2} \ . \qquad (A8)$$

---

*Present address: Philips Medical Systems, Inc., 710 Bridgeport Ave., Shelton, Conn. 06484.

†Present address: Dept. of Physics, Saint Louis University, 221 North Grand Boulevard, St. Louis, Mo. 63103.

[1]H. W. Jackson (unpublished).

[2]L. Onsager, Nuovo Cimento, Suppl. 2, 249 (1949).

[3]R. P. Feynman, in *Progress in Low Temperature Physics*, edited by C. J. Gorter (North-Holland, Amsterdam, 1955), Vol. I, p. 17.

[4]L. Van Hove, Phys. Rev. 95, 249 (1954).

[5]G. V. Chester, R. Metz, and L. Reatto, Phys. Rev. 175, 275 (1968).

[6]G. W. Rayfield and F. Reif, Phys. Rev. 136, A1194 (1964).

[7]B. L. Henson (private communication).

[8]G. Winterling, F. S. Holmes, and T. J. Greytak, Phys. Rev. Lett. 30, 427 (1973).

[9]C. J. Palin, W. F. Vinen, and J. M. Vaughan, J. Phys. C 5, L139 (1972).

[10]A. G. Tweet, Phys. Rev. 93, 15 (1954).

[11]C. F. A. Beaumont and J. Reekie, Proc. R. Soc. Lond. A 228, 363 (1955).

[12]L. Goldstein and J. Reekie, Phys. Rev. 98, 857 (1955).

[13]W. L. Gordon, C. H. S. Shaw, and J. G. Daunt, J. Phys. Chem. Solids 5, 117 (1958).

[14]E. K. Achter and L. Meyer, Phys. Rev. 188, 291 (1969).

[15]R. B. Hallock, Phys. Rev. Lett. 23, 830 (1969).

[16]R. B. Hallock, Phys. Rev. A 5, 320 (1972).

[17]A. D. B. Woods, Phys. Rev. Lett. 14, 355 (1965).

[18]R. A. Cowley and A. D. B. Woods, Can. J. Phys. 49, 177 (1971).

[19]M. Abramowitz and I. Stegun, *Handbook of Mathematical Functions* (Dover, New York, 1965), p. 485.

[20]Reference 19, p. 439.